sciendo
Journal of Electrical Bioimpedance
JoEB
bioimpedance.net

J Electr Bioimp, vol. 9, pp. 176-183, 2018
Received 18 Dec 2018 / published 28 Dec 2018
https://doi.org/10.2478/joeb-2018-0022

Use of a conical conducting layer with an electrical impedance probe to enhance sensitivity in epithelial tissues

Muhammad Abdul Kadir [1,2] and K. Siddique-e Rabbani [1,2]

1. *Department of Biomedical Physics and Technology, University of Dhaka, Dhaka 1000, Bangladesh*
2. *E-mail any correspondence to: kadir@du.ac.bd or rabbani@du.ac.bd*

Abstract

Tetra-polar electrical impedance measurement (TPIM) with a square geometry of electrodes is useful in the characterization of epithelial tissues, especially in the detection of cervical cancer at precancerous stages. However, in TPIM, the peak planar sensitivity just below the electrode surface is almost zero and increases to a peak value at a depth of about one third to one half of the electrode separation. To get high sensitivity for the epithelial layer, having thicknesses of 200 µm to 300 µm, the electrode separation needed is less than 1 mm, which is difficult to achieve in practical probes. This work proposes a conical conducting layer in front of a pencil like probe with a square geometry of TPIM electrodes to create virtual electrodes with much smaller separation at the body surface, thus increasing the sensitivity of the epithelial tissues. To understand the improvements, if any, 3D sensitivity distribution and transfer impedance were simulated using COMSOL Multiphysics software for a simplified body tissue model containing a 300 µm epithelial layer. It has been shown that fractional contribution of an epithelial layer can be increased several times placing a cylindrical conducting layer in between the tissue surface and the electrodes, which can further be enhanced using a conical conducting layer. The results presented in this paper can be used to choose an appropriate electrode separation, conducting layer height and cone parameters for enhanced sensitivity in the epithelial layer.

Keywords: Bioimpedance; Sensitivity; Epithelial tissue; virtual electrode; EIS; Impedance probe; conducting layer.

Introduction

Recent studies demonstrated that there is a great potential of using Electrical impedance spectroscopy (EIS) [1] in the characterization of epithelial tissues. EIS has been successful in the detection of cervical cancer in the preliminary stages [2-4]. Electrical impedance measurement techniques have also been useful in the study of many other epithelial tissues including oral mucosa [5, 6], esophagus [7,8], skin cancer [9] and skin hydration status [10].

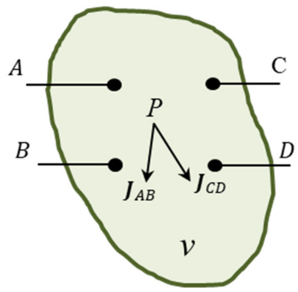

Fig.1: Schematic of current density vectors at point P for two pairs of electrodes AB and CD placed on the surface of a volume conductor.

For these studies, tetra-polar electrical impedance measurement (TPIM) technique is the usual choice as it can eliminate skin contact impedance. In TPIM, for a square geometry of electrodes as shown in figure 1, an alternating current *I* of constant amplitude is applied to a volume conductor *v* though a pair of electrodes *AB* and the resulting voltage drop is measured across another pair of electrodes *CD*. The sensitivity *S* at a point *P* within the volume conductor contributing to the transfer impedance thus measured is defined as [11, p-188],

$$S = \frac{J_{AB} \cdot J_{CD}}{I^2} \quad (1)$$

where $\boldsymbol{J}_{AB}$ and $\boldsymbol{J}_{CD}$ are the current density vectors at the point *P* due to current driven through electrode pairs *AB* and *CD* respectively. If σ is the conductivity at point *P*, the contribution of the point to the transfer impedance z_P is given by,

$$z_P = \frac{1}{\sigma} \cdot \frac{J_{AB} \cdot J_{CD}}{I^2} \quad (2)$$

The total transfer impedance is given by the volume integral of z_p over the whole volume. Any variation in conductivity at any point in the region is automatically addressed through this equation.

For the study of sensitivity at epithelial layers it is useful to analyze the contribution of whole planes in 2D. For any plane passing through point *P*, the contribution of the plane to the total transfer impedance may be obtained through a 2-dimensional integration of equation 2 over this plane. It has been found that for a TPIM the average impedance sensitivity over a plane parallel to the electrode plane just below the surface is almost zero [12]. This is because of the presence of negative sensitive regions in between the current drive and voltage pickup electrodes [13] which cancel out the positive sensitivity in this plane. The negative sensitivity diminishes with depth faster than the decrease in positive sensitivity away from the electrode plane [14]. In tetra-polar impedance measurement with square electrode configuration, negative sensitivity regions extend down to about one-third the drive-receive electrode spacing [15]. For this reason the average sensitivity over planes parallel to the electrode plane increases with depth, reaches a maximum and then falls off gradually. The depth at which the average sensitivity is maximum is approximately one third of the separation between two adjacent electrodes for a square configuration [12]. This indicates that the contribution of the tissue just below the electrode plane to the total transfer impedance is very low. This is a great problem in the bioimpedance measurements of epithelial tissues. In the cervical cancer detection studies [2-4], the electrode separation was chosen to be around a practical minimum of $1\ \mathrm{mm}$ for which the maximum impedance sensitivity occurs at a depth of about $300\ \mu m$ of the cervical tissue. Tissue layers around this depth contributes more to the measured impedance [16]. However, the target depths are usually much smaller. For example, the thickness of epithelial tissue in the ectocervix is between 200 μm and 300 μm under normal and pathological conditions [17]. Therefore, to get increased contribution of the epithelial layer to the measured transfer impedance, the peak sensitivity should be kept around 100 μm to 150 μm. This requires the electrode separation to be very small, of the order of 300 μm to 500 μm (0.3 mm to 0.5 mm), which is very difficult to achieve in practice. Moreover, to achieve very small electrode separation, the area of the electrodes need to be very small as well. This results in higher current density and tissue burn because of Joule heating. To address these limitations, an ingenious method was to shift the electrode plane beyond the skin surface through the interposition of a conducting gel layer [18], so that the peak planar sensitivity occurs in the superficial epithelial layers, the gel taking up the region with the negative sensitivity. This study used electrodes of 1 mm diameter with separations of about 1 mm and 2 mm respectively for measurements on a human hand, with a 1 mm thick hydrogel separator. However, in a low resource country perspective, making such small probes may pose some challenge. Larger electrodes with a larger electrode separation could be more convenient to fabricate, but this will require a thicker gel to get a peak sensitivity at the human tissue interface, which on the other hand, will reduce the sensitivity within the target tissue as most of the current will be contained within the conducting gel layer.

To get around this problem this paper describes a novel idea of using a conical conducting layer in front of a pencil like electrode probe to reduce the effective electrode separation at the surface of the human tissue, giving rise to a new concept of 'virtual electrodes'. Here the outside of the conducting layer is bound unlike the almost infinite extension in 2D used in the above work. In this work, FEM simulation using COMSOL has been used to study the resulting improvements, if any.

The concept of virtual electrodes

The concept is explained with the help of figure 2.

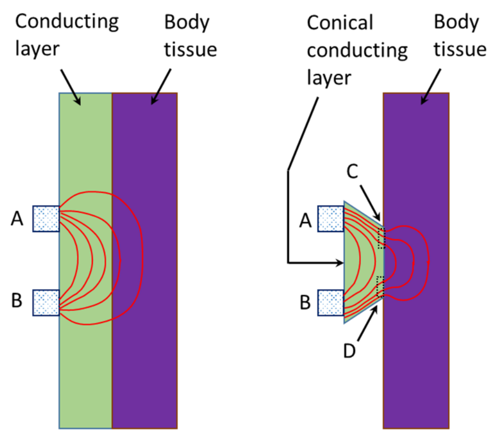

Fig. 2: Schematic representation of the effect of an interposed conducting layer through imaginary current line patterns: a) for a 2D infinite layer, b) for a conical finite layer, giving rise to virtual electrodes with reduced separation.

The figure on the left represents the interposing conducting gel layer, as proposed by reference 18, between the body tissue and the electrode pair *AB*, through which a current is driven from an external current source. Assuming the conducting layer and the body tissue to have the same conductivity, the imaginary current line patterns will be that for a dipole and are represented schematically by the red lines. The figure on the right shows a conical conducting layer of finite dimensions such that it just covers the electrode pair *AB*, as proposed in the present work. The current lines will now be squashed within the conducting layer due to the conical boundary. As soon as these lines reach the infinitely large body volume, these will spread out in an approximate pattern as shown schematically here. Looking from the body volume, it will appear as though the current lines have originated from electrodes within the boundaries of the conical surface touching the body tissue. These have been shown as virtual electrodes *C* and *D* on the right hand diagram in figure 2. Intuitively, these virtual electrode pair *CD* will have a separation much reduced than that of the original electrode pair *AB*. Even if the boundary is not conical, due to concentration of the current within the bounded region and expansion on reaching the underlying unbounded region, current patterns may be expected that will effectively create virtual electrodes with effective reduced separation at the body tissue surface. This is the basis of the present work and is aimed at studying the effects on the sensitivities in planes at different depths within a volume conductor for different shapes and thicknesses of the interposing conducting layer.

Materials and methods

In this study the impedance sensitivity distribution for Tetrapolar electrical impedance measurements on a biological volume for a square geometry of electrodes as shown in figure 1 was simulated using a finite element method (FEM) based software, COMSOL Multiphysics®. A cube of edge length $50mm$ was modeled as a volume conductor representing body tissue as shown in figure 3.

The electrical conductivity (σ) and relative permittivity (ε_r) of the volume conductor were assigned the values of $0.53699\ S/m$ and 17594 respectively, same as for human cervical tissue at 10 kHz [19]. Cylindrical electrodes of 1 mm diameter and 1 mm height were placed on a surface (*xy plane*) of the volume conductor centrally. The circular areas of the cylinders are in contact with the volume conductor. For the initial studies the edge to edge separation between two adjacent electrodes was chosen as $1\ mm$ (center to center separation: $2\ mm$). The bottom diagram of figure 3 shows a zoomed view of the electrodes, on the surface of the modeled volume conductor. Electrodes were modeled as a highly conducting metal having conductivity and permittivity of $1e^6\ S/m$ and 1 respectively. Within the volume conductor representing the body tissue, a thin layer of thickness $300\ \mu m$ just below the electrodes was partitioned to represent epithelial layer (shown green), for calculation of the fractional contribution of this layer to the total measured impedance, but having the same electrical parameters as the bulk volume.

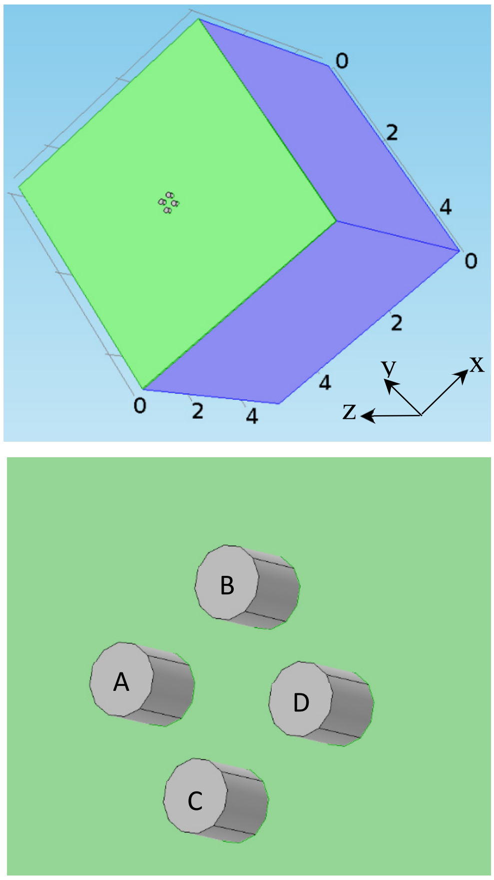

Fig.3: FEM model of biological tissue for computation of impedance sensitivity. Four 1 mm dia cylindrical electrodes with edge to edge separation of 1 mm (centre to centre separation: 2 mm) are placed centrally on a surface of a cubic volume conductor with 50 mm sides. The green layer of thickness 300 µm represents an epithelial layer. A zoomed view of the electrodes is shown at the bottom.

For calculating 3D sensitivity distribution within the volume conductor, a current of unit amplitude (= 1 A) was introduced through the electrode pair *AB* using the *electric current (ec)* interface of AC/DC module in COMSOL Multiphysics. Simultaneously reciprocal current of same amplitude was introduced through another electrode pair *CD*. The study was performed in the frequency domain at10 kHz.

The governing equations for the FEM computations are,

$$\boldsymbol{\nabla}.\boldsymbol{J} = \boldsymbol{Q_j} \quad (3)$$

$$\boldsymbol{J} = (\boldsymbol{\sigma} + \boldsymbol{j\omega\varepsilon_0\varepsilon_r})\boldsymbol{E} + \boldsymbol{J_e} \quad (4)$$

$$\boldsymbol{E} = -\boldsymbol{\nabla V} \quad (5)$$

where, ***J***, Q_j, σ, ω, ε_0 , ε_r , ***E*** and V are the current density, current source, electrical conductivity, angular frequency, permittivity in free space, relative permittivity of the material, electric field and electric potential respectively.

J_e is the external source current density (there is none in the present model).

If $\boldsymbol{n}$ is the unit vector perpendicular to the boundary surface, the boundary condition for the model is

$$\boldsymbol{n}.\boldsymbol{J} = 0 \tag{6}$$

Boundary conditions were set so that the current density on the outer boundary of the volume conductor is zero whereas the boundaries between internal domains satisfy continuity. The meshing tool in COMSOL Multiphysics was used to generate 3D mesh grid in the geometric model. Software controlled *finer* mesh having 446619 tetrahedral elements was used for computation of sensitivity values. The *impedance sensitivity* at a point within the volume conductor was then calculated using equation 2.

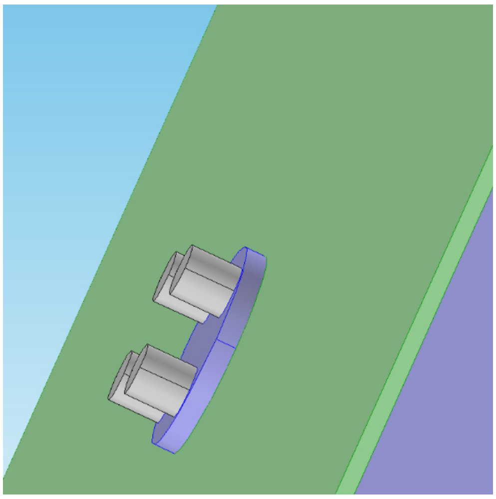

Fig.4: Cylindrical conducting layer material placed in between the electrodes and the epithelial layer. The green layer of thickness 300 µm represents an epithelial layer.

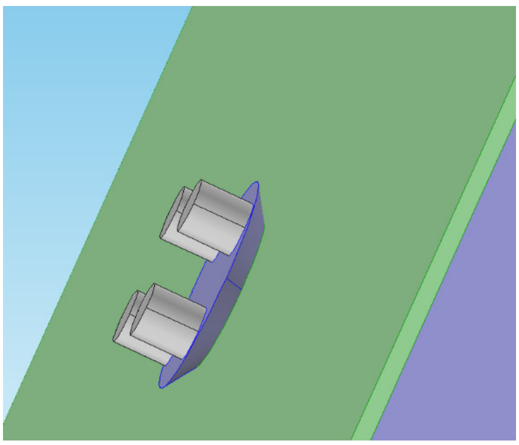

Fig.5: Conical shaped conducting layer placed in between the electrodes and tissue surface.

Although the main motivation of the present work was to study the effect of a conical interposed conducting layer, a cylindrical shape was first studied in order to have an understanding of the new concept. A cylindrical object of 4 mm diameter and 0.4 mm height was interposed between the four electrodes and the body volume as shown in figure 4. The conductivity and permittivity of the conducting layer were taken to be the same as that of the body tissue (human cervix). The distribution of impedance sensitivity within the body volume was computed following equation 2 for different heights of the conducting layer.

The total transferred impedance of the modeled tissues (body tissue+epithelial layer+conducting layer) was computed as [11]:

$$Z_{total} = \int_{v_t} \frac{1}{\sigma} \left(\frac{J_{AB} \cdot J_{CD}}{I^2} \right) dv \tag{7}$$

where the integration is over the whole volume v_t of the tissue and the interposing layer.

Similarly, the contribution of the assumed 300 µm epithelial layer to the transferred impedance was computed as:

$$Z_{el} = \int_{v_{el}} \frac{1}{\sigma} \left(\frac{J_{AB} \cdot J_{CD}}{I^2} \right) dv \tag{8}$$

where the integration is over the volume of the epithelial layer, v_{el} only.

The fractional contribution of the epithelial layer to the total transfer impedance was defined as

$$Fractional\ Impedance = \frac{Z_{el}}{Z_{total}} * 100\ \% \tag{9}$$

A higher value of fractional impedance indicates a higher effective sensitivity of the epithelial layer and is desired for impedance measurements of epithelial layer minimizing contribution from the remaining tissues.

Subsequently, the study was repeated for different conical shapes and thicknesses of the interposing conducting layer, as shown in figure 5, to determine which parameters give the most contribution from the epithelial layer in the total transferred impedance. If the radius of the conducting layer surface touching the electrodes is R_e and that on the other side touching the body tissue is R_t, then the ratio or radii R_t/R_e represents the steepness of the conical segment of the conducting layer. For the study, the ratio was varied by changing R_t only; R_e was kept fixed. This gives varied conical shapes of the interposing layer, which includes cylindrical shape as well, when the value of the ratio would be unity. A conical conducting layer is shown in figure 5, which has a radii ratio of less than unity. However, the study was also extended to an inverse conical shape, where the radii ratio is slightly greater than unity. The fractional impedance of the epithelial layer was computed for different thicknesses of the conical conducting layer corresponding to different values of the radii ratio. Similar measurements were simulated for larger electrode separations as well.

From a practical point of view, a conical conducting layer has the advantage that it can be made of conducting rubber and inserted inside a detachable attachment, to be slipped over the tip of a pencil like probe having permanent electrodes. Thus, it can be made as a low cost disposable tip eliminating cross infection while taking measurements on different persons. In such a device, a rubber layer of thickness of about one mm would be suitable for handling. Therefore, the maximum fractional contribution of a 300 µm epithelial layer was studied for a fixed conducting layer thickness of 1.2 mm, but for different electrode separations and varying radii ratio.

Ethical approval

The conducted research is not related to either human or animal use

Results

Figure 6 shows the average sensitivity values over planes parallel to the electrode plane within the 50 mm cubic volume conductor for a cylindrical conducting layer of 4 mm diameter (as shown in figure 4). Here depth indicates the distance of a plane of interest from the surface of the tissue and the interposing conducting layer is referred to as a ‘bolus’. Depth zero indicates the body surface with or without an interposing conducting layer (or bolus). The edge-to-edge electrode separation was 1 mm (center to center electrode separation: 2 mm). The depths of the planes were taken in steps of 0.1 mm; there were 250000 values in each plane. Average sensitivity over a plane was then calculated by dividing the sum of sensitivity values at all points in that plane divided by the number of points.

Figure 7 shows the variation of fractional impedance of the epithelial layer against conducting layer height for an edge-to-edge electrode separation of 1 mm (center to center: 2 mm). It has a maximum at a conducting layer height of 0.4 mm.

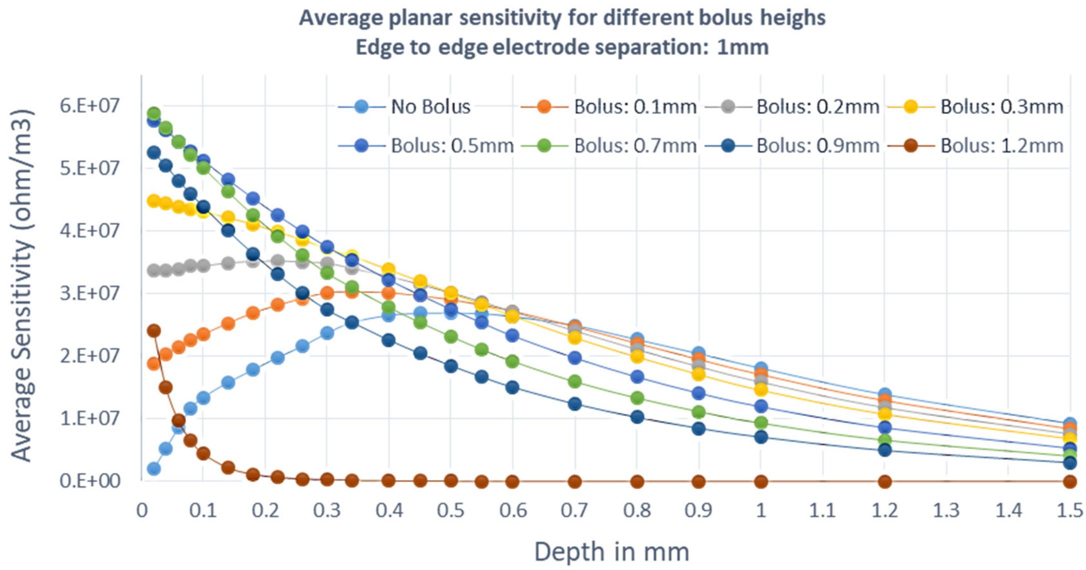

Fig.6: Variation of plane average sensitivity along depth with different conducting layer (bolus) height for edge to edge electrode separation of 1mm. Depth zero indicates the surface of the volume conductor with or without the interposing conducting layer (probe).

Figure 8 shows the variation of fractional impedance of the epithelial layer against radii ratio of the conical conducting layer for different heights of the conducting layer (bolus height). In this case, the electrode separation was 1 mm (edge-edge) and the diameter of the side of the conical conducting layer touching the electrodes was kept constant at 4 mm. Figure 9 shows similar curves but for a larger separation between the electrodes. In this case the diameter of the conical conducting layer surface touching the electrodes was 6 mm and the edge-to-edge electrode separation was 2 mm (center-to-center: 3 mm).

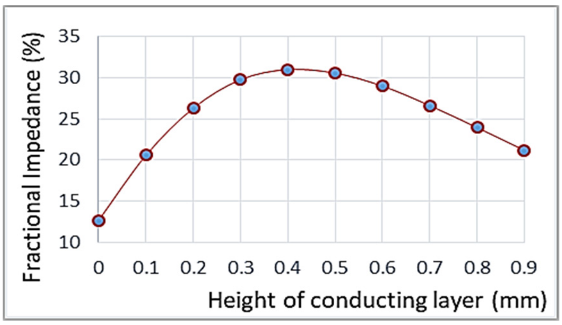

Fig.7: Fractional impedance of the epithelial layer compared to the whole tissue as a function of the height of conducting layer. Edge-edge electrode separation is 1 mm.

Finally, figure 10 shows the variation of fractional impedance of the epithelial layer with conical bolus radii ratio for different electrode separation (edge to edge) while the bolus height was kept constant at 1.2 mm.

Discussion

The proposal for a conical interposing layer is novel and was proposed based on an intuitive visualization as shown in figure 2. It has been borne out through the simulations carried out in the present work. The concept of virtual electrodes is again a new one and may have wider applications.

Coming to the results obtained in the present work, it can be observed from figure 6 that without any conducting layer, the fractional impedance of the epithelial layer of thickness $300\ \mu m$ is only 12% of the total impedance. However, fractional impedance of the epithelial layer can be increased to about 30% using a cylindrical conducting layer of 0.4 mm height for an edge-to-edge electrode separation of 1 mm. An optimum height of conducting layer for enhanced sensitivity in the epithelial layer may be chosen based on the electrode separation.

It can also be observed from figure 6 that the average sensitivity is almost zero at the surface of the volume conductor without any conducting layer (no bolus), which agrees with previous studies [16]. The planar average sensitivity increases with depth, reaches a maximum and then decreases again gradually at higher depths. The peak sensitivity occurs at about 0.5 mm, which is half the edge to edge electrode separation and one fourth of the centre to centre separation, which also agrees approximately with the findings of other workers [12, 15]. For increasing height of conducting layer (bolus height), the average sensitivity at the surface of the volume conductor (depth = 0) increases because of a shift of the low sensitivity region into the interposing conducting layer. It is evident from figure 6 that the depth of the peak sensitivity shifts towards the surface of the volume conductor with increasing height of conducting layer, as expected. However, the average impedance sensitivity near the surface increases with increasing conducting layer height initially but decreases after a certain height of the conducting layer. This indicates that there is an optimum height of the conducting layer for which the sensitivity just below the surface (epithelial layer) is maximum, which is about 0.7 mm in this case. From an intuitive standpoint, this should not have been the case for an interposing conducting layer with infinite extension, as used by reference 18. In this case, the differences would be only through a leftward shift of the curve (for which the conducting layer thickness is zero); the sensitivity at the surface of the body tissue would be decreasing monotonically.

Therefore, it is obvious that the observed changes are because of the finite and bounded conducting layer which confines the current paths. Once the current paths reach the large body volume, these spread out afresh, as if the current is originating from electrodes with a much smaller separation at the surface. This gives rise to the concept of 'virtual electrodes' as shown in figure 2. Again in figure 6, for a bolus height of 1.2 mm, there is a sudden drop with depth compared to that for a bolus height of 0.9 mm. This may be explained from a perspective of current line distributions shown in figure 2. For a bolus height of 1.2 mm, most of the current lines are concentrated within the interposing layer, very little goes into the body tissue underneath, which is not the case for the lower values of bolus heights. This also points out that if one wants to study the first 50 μm or so of the epithelial layer, such a configuration may be useful where the volume below contributes very little.

Figure 7 indicates that the fractional contribution of the simulated 300 μm epithelial layer increases with increasing height of conducting layer, reaches a maximum and then falls gradually. In the present case, for an edge to edge electrode separation of 1 mm, the optimum height of conducting layer for which the contribution of the epithelial tissue to the total impedance is maximum (about 30%) is found to be 0.4 mm. This result is a consequence of the phenomena observed in figure 6. It should be noted that the optimum height of the conducting layer will depend on the electrode separation.

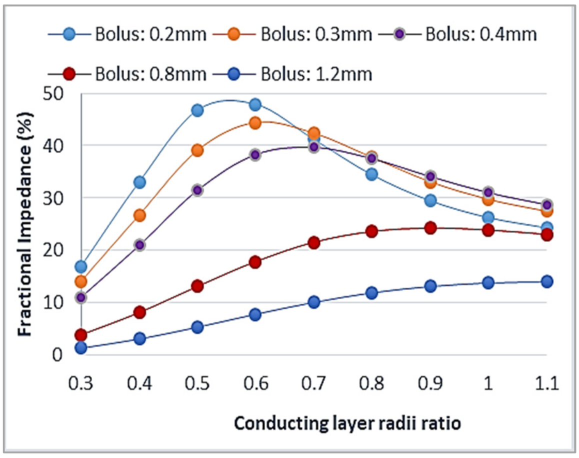

Fig.8: Fractional contribution of the epithelial layer to the total transfer impedance against radii ratio of the conical conducting layer for different conducting layer height. Edge to edge electrode separation is 1 mm.

Figure 8 relates to conical conducting layers, the main proposition that this work started off with. Here a radii ratio of 1 corresponds to the cylindrical conducting layer discussed above and the radii ratio decreases for the conical configuration under study in the present work. It can be seen that for any fixed thickness of the conducting layer, as the radii ratio decreases from unity, corresponding to increased angle of the cone, the fractional contribution of the epithelial layer increases, supporting the intuitive proposition of this work that the separation of the 'virtual electrodes' decreases with increasing angle of cone. However, below a certain value of radii ratio the fractional contribution decreases. This may be due to too steep cone angles so that most of the current is confined to interposing conducting layer rather than the body volume.

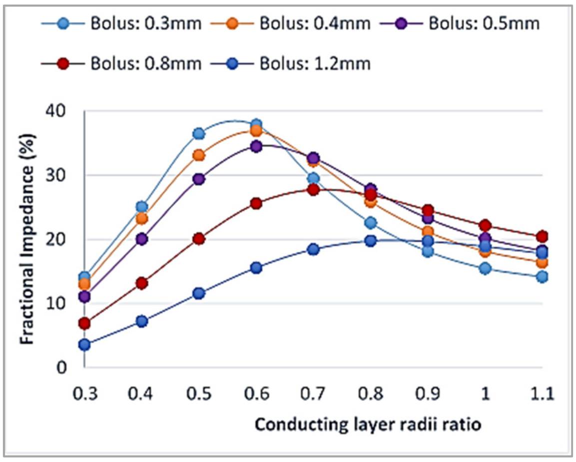

Fig.9: Fractional contribution of the epithelial layer to the total transfer impedance against radii ratio of the conical conducting layer for different conducting layer height. Edge to edge electrode separation 2mm.

Figure 8 shows that the 300 µm epithelial layer contributes to about 50% of the measured impedance for a conducting layer height of 0.2 mm (200 µm) corresponding to a radii ratio of a little over 0.5, which is the maximum among those studied in this work. This is relevant to a conical conducting layer with a diameter of 4 mm at the electrode surface and a little over 2 mm at the body surface, for a height of 0.2 mm. The edge to edge electrode separation is 1 mm (centre to centre: 2 mm) in this case. The peak contribution of the 300 µm epithelial layer for a larger electrode separation (edge to edge: 2 mm, centre to centre: 3 mm) is slightly less as shown in figure 9. This corresponds to a conical conducting layer with a diameter of 6 mm at the electrode surface and about 3.5 mm at the body surface, for a height of 0.3 mm. The peak contribution is a little less than 40%. In figure 8, for the same height (0.3 mm) the peak value was about 45%, slightly more.

The cone shapes with radii ratio of about 0.5 and heights of 0.2 to 0.3 mm as required by the results of the present study may sometime be difficult to configure with accuracy. A layer height of about 1 mm could be handled better, particularly if using conducting rubber as mentioned before. Figure 10 shows that for a layer height of 1.2 mm, the maximum contribution of the 300 µm epithelial layer is rather less, at about 20%, and which can be achieved for any electrode separation between 3 mm and 6 mm for radii ratio between 0.7 and 0.9. Although the contribution is reduced, this arrangement could be achieved easily in a more practical device.

The fractional impedance of the epithelial layer was computed considering a thickness of 300 µm. The fractional impedance values need to be interpreted with care for other thickness of epithelial layers under consideration. It should also be noted that the fractional impedance values will be different if the dielectric properties of the conducting layer material are different than that of the tissue under investigation (cervical tissue in the current study).

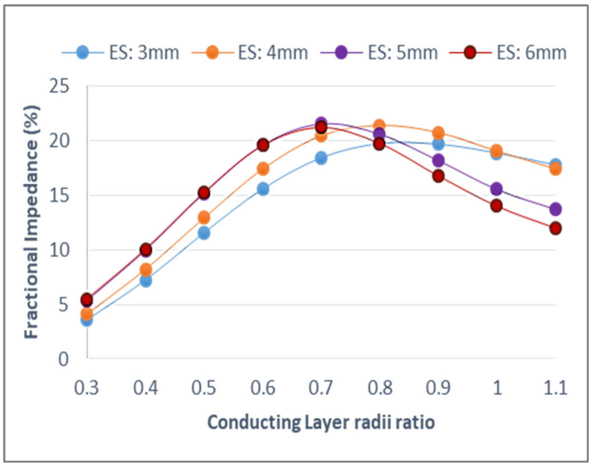

Fig.10: Variation of fractional impedance of the epithelial layer with conical bolus radii ratio for different electrode separations (edge to edge) while the bolus height was constant at 1.2 mm.

In conclusion, to overcome the problem of very low impedance sensitivity at epithelial layer with a practically implementable tetra-polar impedance probe, the utility of a conical conducting layer for enhancement of impedance sensitivity in epithelial tissues has been proposed that is easily implementable as a pencil like probe. The results presented in this paper can be used to choose an appropriate electrode separation, conducting layer height and conducting layer radii ratio for enhanced sensitivity in the epithelial layer.

Although reference 18 used a conducting gel as the interposing layer, it could be any suitable material. A conducting rubber would be preferred for the conical system as this could be handled better in a practical probe, may be with a thin layer of conducting gel on both sides. Thus it could form part of a disposable tip, slipping over a pencil like probe with permanent electrodes. This would be hygienic and cost effective eliminating the chances of cross infection while measuring multiple patients using the same probe.

Competing interests

The authors declare that they have no competing interests.

Acknowledgement

International Science Program (ISP) of Uppsala University, Sweden is acknowledged for financial supports.

References

1. Bertemes-Filho P. Electrical Impedance Spectroscopy. Bioimpedance in Biomedical Applications and Research: Springer; 2018. p. 5-27. https://doi.org/10.1007/978-3-319-74388-2_2
2. Abdul S, Brown B, Milnes P, Tidy J. A clinical study of the use of impedance spectroscopy in the detection of cervical intraepithelial neoplasia (CIN). Gynecologic Oncology. 2005;99(3):S64-S6. https://doi.org/10.1016/j.ygyno.2005.07.046
3. Abdul S, Brown B, Milnes P, Tidy J. The use of electrical impedance spectroscopy in the detection of cervical intraepithelial neoplasia. International Journal of Gynecological Cancer. 2006;16(5):1823-32. https://doi.org/10.1111/j.1525-1438.2006.00651.x
4. Brown BH, Milnes P, Abdul S, Tidy JA. Detection of cervical intraepithelial neoplasia using impedance spectroscopy: a prospective study. BJOG: An International Journal of Obstetrics & Gynaecology. 2005;112(6):802-6. https://doi.org/10.1111/j.1471-0528.2004.00530.x
5. Murdoch C, Brown BH, Hearnden V, Speight PM, D'Apice K, Hegarty AM, et al. Use of electrical impedance spectroscopy to detect malignant and potentially malignant oral lesions. International journal of nanomedicine. 2014;9:4521. https://doi.org/10.2147/IJN.S64087
6. Tatullo M, Marrelli M, Amantea M, Paduano F, Santacroce L, Gentile S, et al. Bioimpedance detection of oral lichen planus used as preneoplastic model. Journal of Cancer. 2015;6(10):976. https://doi.org/10.7150/jca.11936
7. González-Correa C, Brown B, Smallwood R, Kalia N, Stoddard C, Stephenson T, et al. Virtual biopsies in Barrett's esophagus using an impedance probe. Annals of the New York Academy of Sciences. 1999;873(1):313-21. https://doi.org/10.1111/j.1749-6632.1999.tb09479.x
8. Weijenborg PW, Rohof WO, Akkermans LM, Verheij J, Smout AJ, Bredenoord AJ. Electrical tissue impedance spectroscopy: a novel device to measure esophageal mucosal integrity changes during endoscopy. Neurogastroenterology & Motility. 2013;25(7):574-e458. https://doi.org/10.1111/nmo.12106
9. Aberg P, Nicander I, Hansson J, Geladi P, Holmgren U, Ollmar S. Skin cancer identification using multifrequency electrical impedance-a potential screening tool. IEEE transactions on biomedical engineering. 2004;51(12):2097-102. https://doi.org/10.1109/TBME.2004.836523
10. Martinsen ØG, Grimnes S, Karlsen J. Electrical methods for skin moisture assessment. Skin Pharmacology and Physiology. 1995;8(5):237-45. https://doi.org/10.1159/000211353
11. Grimnes S, Martinsen ØG. Bioelectricity and bioimpedance basics. 2nd ed: Academic Press; 2008.
12. Brown B, Wilson A, Bertemes-Filho P. Bipolar and tetrapolar transfer impedance measurements from volume conductor. Electronics Letters. 2000;36(25):2060-2. https://doi.org/10.1049/el:20001439
13. Grimnes S, Martinsen ØG. Sources of error in tetrapolar impedance measurements on biomaterials and other ionic conductors. Journal of Physics D: Applied Physics. 2006;40(1):9. https://doi.org/10.1088/0022-3727/40/1/S02
14. Kadir MA. Development of a multi-frequency system for medical application of Focused Impedance Method (FIM). Doctoral dissertation, University of Dhaka; 2018 http://repository.library.du.ac.bd:8080/handle/123456789/1245
15. Islam N, Rabbani KS, Wilson A. The sensitivity of focused electrical impedance measurements. Physiological measurement. 2010;31(8):S97. https://doi.org/10.1088/0967-3334/31/8/S08
16. Brown BH, Tidy JA, Boston K, Blackett AD, Smallwood RH, Sharp F. Relation between tissue structure and imposed electrical current flow in cervical neoplasia. The Lancet. 2000;355(9207):892-5. https://doi.org/10.1016/S0140-6736(99)09095-9
17. Ghosh I, Mittal S, Banerjee D, Chowdhury N, Basu P. Study of Correlation of Cervical Epithelial Thickness With the Grade of Colposcopic Abnormality. International Journal of Gynecological Pathology. 2016;35(3):269-74. https://doi.org/10.1097/PGP.0000000000000249
18. Bertemes-Filho P, Brown BH, Smallwood RH Wilson AJ, Stand-off electrode (SoE): a new method for improving the sensitivity distribution of a tetrapolar probe, Physiological Measurement. 2003; 24:517–525. https://doi.org/10.1088/0967-3334/24/2/362
19. Andreuccetti D FR, Petrucci C. An Internet resource for the calculation of the dielectric properties of body tissues in the frequency range 10 Hz - 100 GHz 1997. Available from: Website at http://niremf.ifac.cnr.it/tissprop/. IFAC-CNR, Florence (Italy).